Local disorder studied in $SrTiO_3$ at low temperature by EXAFS spectroscopy

M. Fischer and A. Lahmar
Département de Recherches Physiques, Université Pierre et Marie Curie, T22 E4, 4 Place Jussieu, F-75252 Paris Cedex 05, France

M. Maglione
Laboratoire de Physique du Solide, Université de Bourgogne, Boîte Postale 138, 21004 Dijon Cedex, France

A. San Miguel, J. P. Itié, and A. Polian
Laboratoire de Physique des Milieux Condensés, Université Pierre et Marie Curie, T13 E4, 4 Place Jussieu, F-75252 Paris Cedex 05, France

F. Baudelet
Laboratoire pour l'Utilisation du Rayonnement Electromagnétique, Université Paris-Sud, Bâtiment 209d, F-91405 Orsay Cedex, France
(Received 16 July 1993; revised manuscript received 1 November 1993)

The temperature dependence of the local distortions in $SrTiO_3$ has been studied by EXAFS spectroscopy at the titanium K edge (4982 eV). The oxygen-ion Debye-Waller factor σ_0^2 has been determined from 4.5 to 240 K. The antiferrodistortive transition at 105 K is evidenced by a step in this Debye-Waller factor. At about 31 K, a maximum of σ_0^2 is detected and the EXAFS oscillations due to the first oxygen shell increase. This is the signature of a maximum disorder in the lattice vibrations in this temperature range. A quasiharmonic model with a sinusoidal modulation of the Ti-O distance cannot account for these observations. The lattice and electronic excitations which could support our data are qualitatively described.

I. INTRODUCTION

X-ray-absorption spectroscopy is currently used to probe lattice distortions in crystalline solids. In ABO_3 perovskites, these distortions may be of two kinds: either a rotation of the oxygen octahedron or a displacement of the central B ion against its oxygen cage. Both effects are successfully investigated by extended x-ray-absorption fine-structure (EXAFS) spectroscopy.[1] In $KTaO_3$:Nb, the ferroelectric phase transition is induced by the Nb^{5+} ions substituted for Ta^{5+} at the center of the oxygen octahedron. A number of experiments have been focused toward the precursor effects of this phase transition. Nuclear magnetic resonance (NMR)[2] and Raman[3] results were explained using a model of polar nanoclusters around each Nb impurity in the cubic phase. However, since the above techniques are sensitive to electric-field gradients or the ionic polarizabilities, the exact origin of the polar clusters was not clear. From EXAFS spectroscopy, it was shown that these clusters may arise from the Nb^{5+} ions being off center in the paraelectric and in the polar phase as well.[4]

The situation is less clear in pure compounds such as barium titanate ($BaTiO_3$), potassium niobate ($KNbO_3$), and potassium tantalate ($KTaO_3$). Detailed EXAFS data would be very helpful in order to get a microscopic insight on the ionic positions in the cubic phase.

In strontium titanate ($SrTiO_3$), the antiferrodistortive transition at 105 K and atmospheric pressure, triggered by a rotation of the oxygen octahedra, has been extensively studied using numerous techniques. However, the number of EXAFS spectroscopy results is very small.[5,6] We showed at the strontium K edge that this phase transition results in a steplike Debye-Waller factor of the first oxygen shell. From the available data so far, precursor order-disorder effects are not detected in EXAFS experiments. On the other hand, at room temperature a new displacive phase of $SrTiO_3$ was induced above 6 GPa.[7] We showed that this phase was very different from the low-temperature antiferrodistortive phase described above. In fact, the high-pressure phase may arise from a static displacement of the central Ti ions and from a rotation of the oxygen octahedra.[8] This statement was based on EXAFS data taken at the strontium K edge. Since the strontium sublattice is not directly involved in the antiferrodistortive process, complementary investigations were necessary. With this aim, we have performed x-ray-absorption experiments at the titanium K edge at low temperature and will focus on this compound in the following.

II. EXPERIMENTAL PROCEDURE

A. Sample preparation

Two kinds of samples were prepared: Small crystallized samples of less than 100 μm in thickness along the [100] direction of the cubic phase, and homogeneous powdered samples obtained by sieving and selecting particles smaller than 5 μm in size. Powder is deposited as a thin layer of constant thickness on self-adhesive tape, and two such superposed preparations were used to process samples with total absorption μ less than 1 and $\Delta\mu$ of 0.3–0.5.

B. EXAFS measurements

The experiments were carried out at DCI LURE (Orsay) with a positron beam energy of 1.85 GeV and a maximum stored current of 320 mA. Data were collected by using a classical two-crystal Si(111) spectrometer. Harmonics were rejected by slightly detuning the monochromator. We measured the absorption spectra of $SrTiO_3$ at the titanium K edge (4982 eV) from 4.5 to 240 K. The maximum error in the temperature measurement is about 1 K. The absorption data were recorded from 4850 to 5750 eV with 1 s accumulation time per point and with 2-eV steps. Data were collected in transmission mode by measurements of the beam intensities I_0 and I, respectively, before and after the sample. Two runs were performed. During the first run, the powdered sample and the crystal were mounted on the same holder. The best results without distortion of spectra were obtained on the powdered samples. Only three crystal spectra were usable (5, 21, and 32 K). The second run was performed only on powdered samples of about 40 μm thickness. At the same time, in order to check that the observed effects are intrinsic in $SrTiO_3$, we recorded the absorption spectra of TiO_2 powdered samples.

C. Data processing

The extended x-ray-absorption fine-structure signal analysis was performed by a procedure which involves complete software written by San Miguel.[9] The oscillatory part of the absorption coefficient is given by

$$\chi(E)=\frac{\mu(E)-\mu_0(E)}{\mu_0(E)} , \tag{1}$$

where $\mu(E)$ is the observed absorption and $\mu_0(E)$ is the atomic absorption. The atomic absorption coefficient $\mu_0(E)$ was approximated by a fifth-degree polynomial. The threshold energy was measured at the inflection point of the edge (Fig. 1).

The oscillatory part of the absorption coefficient above the K edge in the plane-wave single-scattering approximation is given by

$$\chi(k)=\sum_j \frac{N_j}{kr_j^2}|f_j(k,\pi)|e^{-2\sigma_j^2k^2}e^{-2r_j/\lambda}\sin[2\mathbf{k}\cdot\mathbf{r}_j+\psi_j(k)] , \tag{2}$$

where N_j is the number of neighbor atoms at the distance r_j from the absorbing atom, $|f_j(k,\pi)|$ is the backscattering amplitude, σ_j is the Debye-Waller factor of the jth shell, and $\psi_j(k)$ is the total phase shift due to the backscattering and absorbing atoms. λ is the electron mean free path. k denotes the wave number of the photoelectron,

$$k=\hbar^{-1}[2m(E-E_0)]^{1/2} , \tag{3}$$

where E is the energy of the incident photon and E_0 is the threshold energy.

To get information in real space, a Fourier transform (FT) of the $k^n\chi(k)$-weighted data must be made. With $n=3$, the peak of the oxygen shell was well defined. A Kaiser window ($\tau=2.5$) was applied to the $k^3\chi(k)$-weighted data before Fourier transforming. This window was extended from 4.5 up to 13 Å^{-1}. The same Kaiser window was used for each temperature. Fourier transforms at different temperatures are shown in Fig. 2. The first intense peak is due to the first oxygen shell. The two

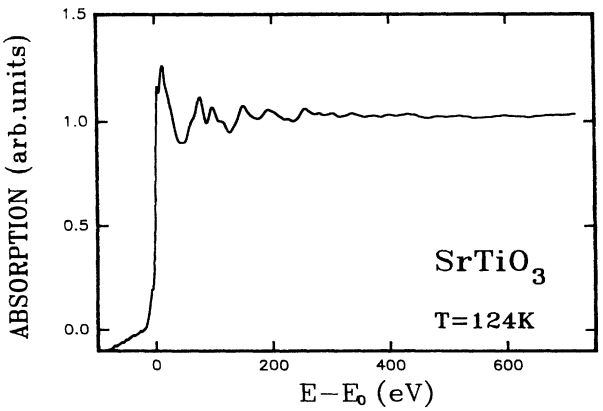

FIG. 1. Normalized x-ray-absorption spectrum of $SrTiO_3$ at 124 K (reference temperature).

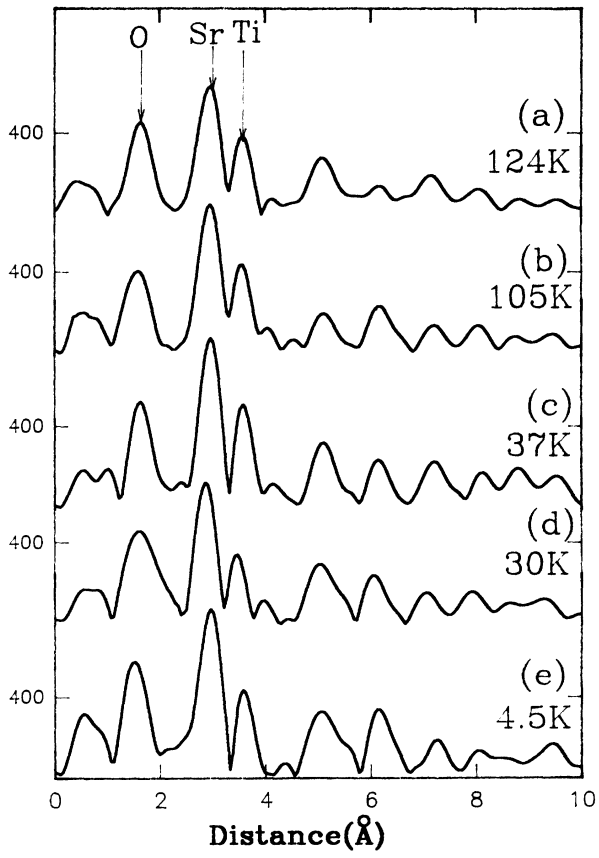

FIG. 2. Amplitudes of fast Fourier transforms of the EXAFS oscillations from the paraelectric phase (124 K) down to 4.5 K. The first peaks at distances shorter than 2 Å are due to some background oscillations in the experimental spectra. Note the broadening of the oxygen peak at 30 K [curve (d)].

following peaks, which are not completely resolved, are essentially due to the first strontium and titanium shells.

In the following, we will focus our attention on the first oxygen peak because in perovskites the plane-wave single-scattering approach can be used essentially for the first atomic shell.[1] To give an interpretation of the farthest peaks collinear double- and triple-scattering contributions must be considered.

In order to determine the temperature dependence of the Debye-Waller factor σ_0, we performed a one-shell fit of the Fourier transform of the oxygen shell (inverse Fourier transform). Because of the very small changes of the lattice parameters with temperature (5×10^{-4} in relative value between 200 and 100 K), the interatomic distances were fixed at the values deduced from x-ray-diffraction measurements.[10]

In these calculations, the oxygen backscattering amplitude $|f_0(k,\pi)|$ and the phase shift $\psi_0(k)$ must be known. These quantities were obtained by using for the first and the second run, respectively, the 124- and the 120-K spectrum as a reference, and the crystallographic data known at these temperatures: the number of oxygen atoms is $N_0=6$ and the interatomic distance is $r_{\text{Ti-O}}=1.9492$ Å. At these temperatures, the σ_0 value was determined theoretically by using a Debye quasiharmonic model (see Sec. III B). N_0, λ, $|f_0(k,\pi)|$, and $\psi_0(k)$ were assumed to be temperature independent.

III. RESULTS AND DISCUSSION

A. Fourier transforms

All the Fourier-transform moduli of the EXAFS spectra exhibit one well-resolved first peak which can be attributed to the six oxygen neighbors (Fig. 2). This peak has the same profile and the same intensity at all the temperatures in the cubic phase. Around 105 K, which is the structural phase-transition temperature, the oxygen peak broadens slightly and its intensity decreases [Fig. 2(b)]. In the tetragonal phase, when the temperature is lowered, the oxygen peak recovers the intensity and profile observed in the cubic phase. During the first run at about 30 K [Fig. 2(d)] this peak becomes broader with a small decrease in intensity. It is interesting to notice that the profiles of the two following peaks, which are mainly due to the Sr and Ti shells, do not change.

The broadenings which are described above cannot be due to a temperature gradient in the cryostat or a temperature change during the data recording. Indeed, the measurements on the crystal and on the powders which were mounted on the same holder at about 5 cm from each other have shown that the temperature gradient is about 0.4 K/cm and the temperature change during the 5-min recording is smaller than 0.5 K. Such temperature changes cannot explain the observed broadenings.

At lower temperatures [Fig. 2(e)], the oxygen peak recovers its sharp profile with a slight increase of its intensity and an important shift of its position. During the second run, the low-temperature anomaly was found close to 32 K. In this run after every measurement on $SrTiO_3$, the EXAFS spectrum of a TiO_2 powdered sample was recorded. The oxygen peak of the TiO_2 (FT) is not broader in this temperature range.

B. Debye-Waller factor

To fit the experimental spectra we have used a reduced form of Eq. (2),

$$\chi_0(k)=\frac{N_0}{kr_{\text{Ti-O}}^2}|f_0(k,\pi)|e^{-2\sigma_0^2k^2}e^{-2r_{\text{Ti-O}}/\lambda}\times\sin[2kr_{\text{Ti-O}}+\psi_0(k)]\ . \tag{4}$$

EXAFS data allow the determination of the temperature dependence of the Debye-Waller factor σ_0 of oxygen ions (Fig. 3). They do not give information on the absolute values. The Debye-Waller factor determined by EXAFS experiments is composed of two contributions: a thermal contribution σ_0^{th} and a static disorder contribution σ_0^{SD}.

Following a procedure which has already been used to explain EXAFS results under pressure,[11] the thermal contribution σ_0^{th} (mean-square relative displacement) was calculated. Using a Debye quasiharmonic approximation, $(\sigma_0^{\text{th}})^2$ is given by the following relation,[11,12]

$$(\sigma_0^{\text{th}})^2=\frac{6\hbar}{M\omega_D}\left[\frac{1}{4}+\left[\frac{T}{\theta_D}\right]^2\Phi_1\right]-\frac{3\hbar}{M\omega_D^3}\psi\ . \tag{5}$$

Here, M is the average mass of Ti and O ions, ω_D is the Debye cutoff frequency, θ_D is the Debye temperature, and T is the absolute temperature. Φ_1 and ψ are integrals given by the two following relations,

$$\Phi_1=\int_0^{\theta_D/T}\frac{x}{e^x-1}dx\ , \tag{6}$$

and

$$\psi=\int_0^{\omega_D}\left[\frac{1+e^{\beta\hbar\omega}}{e^{\beta\hbar\omega}-1}\right]\omega\cos\left[\frac{\omega r_{\text{Ti-O}}q_D}{\omega_D}\right]d\omega\ , \tag{7}$$

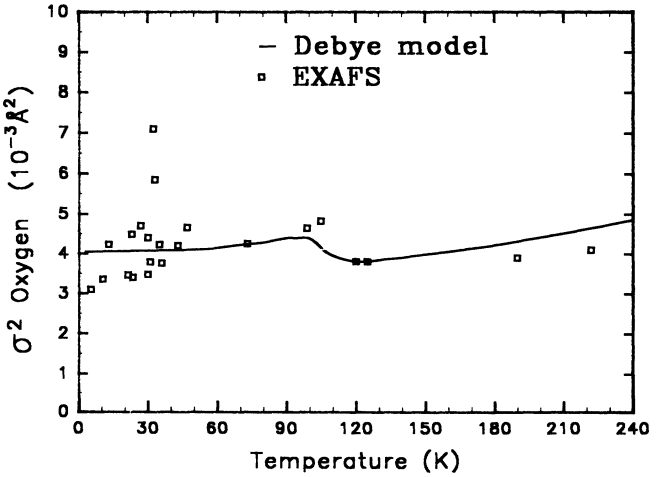

FIG. 3. Oxygen Debye-Waller factor versus temperature in $SrTiO_3$. The full line was computed from a purely Debye model using Eq. (5). The steplike anomaly at 105 K results from the antiferrodistortive transition.

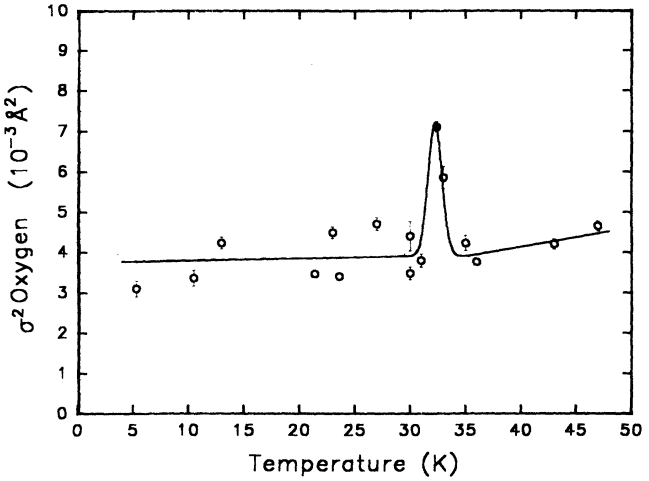

FIG. 4. Temperature dependence of oxygen Debye-Waller factor from 5 to 45 K. The sharp maximum at 31 K is the signature of a strongly non-Debye behavior. The error bars for the Debye-Waller factors are the standard errors. The full line is only a guide for the eyes.

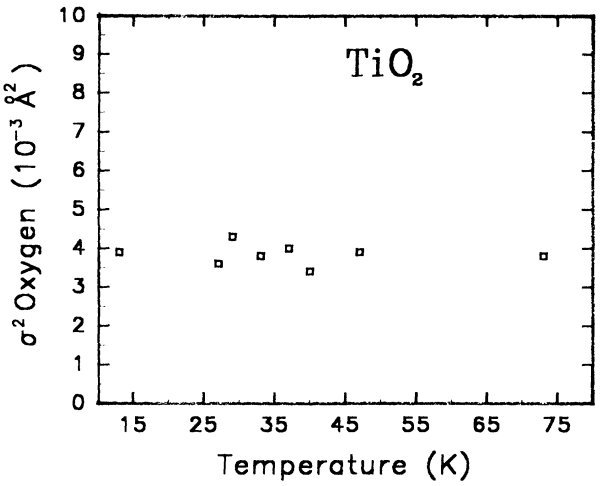

FIG. 5. Oxygen Debye-Waller factor of TiO_2 versus temperature. The standard errors are smaller than 2×10^{-5} Å^2.

where q_D is the Debye wave number.

From the measurements of the elastic constants by Rehwald,[13] a Debye temperature θ_D was calculated at various temperatures by using the Voigt-Reuss-Hill-Gilvarny approximation.[14] The temperature dependence of $(\sigma_0^{th})^2$ is shown in Fig. 3 and compared with the experimental results σ_0^2. Since only the variation of σ_0^2 and not its absolute value is determined, the calculated value at 124 (or 120 K) was taken as a reference for σ_0^2. Consequently, the experimental points of $\sigma_0^2(T)$ are shifted by a constant value of 3.8×10^{-3} Å^2. A decrease of σ_0^2 with temperature was observed with two anomalies, one small at about 105 K and another one stronger around 31 K.

C. Discussion

The comparison between $\sigma_0^2(T)$ and $(\sigma_0^{th})^2$ curves gives information on the static local disorder. From 240 down to 40 K, the differences between the experimental and the calculated values are smaller than 10^{-3} Å^2. Particularly at 105 K the small difference between σ_0^2 and $(\sigma_0^{th})^2$ (0.5×10^{-3} Å^2) shows that the static disorder of oxygen ions due to the TiO_6-octahedra rotation is smaller than 2×10^{-2} Å and the transition is essentially driven by the thermal fluctuations. It should be noted that the shapes of $\sigma_0^2(T)$ and $(\sigma_0^{th})^2$ curves down to 40 K are compatible with the results of molecular-dynamics calculations obtained by Mair to describe the temperature dependence of the mean-square displacement for antiferrodistortive phase transitions.[15]

At about 31 K, a sharp maximum of $\sigma_0^2(T)$ is found (Fig. 4). This peak is about 3.5×10^{-3} Å^2 above the mean value of σ^2 in this temperature range. This is well outside the maximum scatter of the points (1.5×10^{-3} Å^2). This means that a large disorder increases in this temperature range and then disappears for lower temperatures. The high value of $\sigma_0^2(31\text{ K})=7\times10^{-3}$ Å^2 is the signature of a large static disorder or a strong anharmonicity in the Ti-O bonds. In the same temperature range, there is no anomaly in the behavior of the Debye-Waller factor of TiO_2 powders (Fig. 5).

Moreover, even with this high value of σ_0^2, $\chi_0(k)$ is not well fitted (Fig. 6). For the 30-K temperature range, it is necessary to renormalize the oscillation amplitudes to reproduce the experimental spectrum. There are three ways to do so in Eq. (4):

to perturb the terms containing an $r_{Ti\text{-}O}$ contribution;

to increase the electron mean free path λ,

or to increase the oxygen backscattering amplitude f_0.

Extended calculations are needed in order to get a full understanding of these effects. In the following, we will describe qualitative models which can fulfill one of the above conditions. Moreover, these models are all compatible with a strong disorder which is evidenced by the large Debye-Waller factor.

In a first step, the amplitude misfit may arise from ionic distortions. Within a perfect $SrTiO_3$ lattice, we intro-

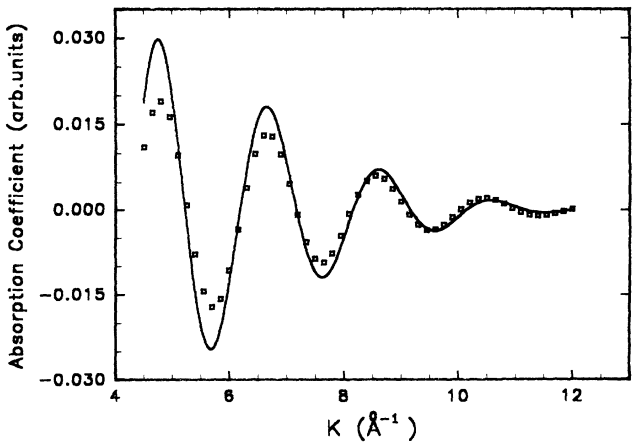

FIG. 6. Experimental (full line) and calculated (open squares) EXAFS oscillations at 30 K of the first oxygen shell in $SrTiO_3$.

duce a sinusoidal modulation of the Ti-O distances,

$$r_{\text{Ti-O}}(n)=r_0+A_n\sin\frac{2\pi na}{\lambda_m}\ , \tag{8}$$

where r_0 is the spatially averaged Ti-O distance, λ_m is the wavelength of the modulation, n is the unit-cell index, and a is the lattice parameter. With this hypothesis, the EXAFS intensity reads

$$\chi_0(k)\sim\frac{N_0}{kr_0^2}|f_0(k,\pi)|e^{-2r_0/\lambda}e^{-2\sigma_0^2k^2}\left\{\frac{1}{N_c}\sum_{n=0}^{N_c-1}\sin\left[2kr_0+2kA_n\sin\frac{2\pi na}{\lambda_m}+\psi_0(k)\right]\right\}\left[1-\frac{2A_n}{r_0}\sin\frac{2\pi na}{\lambda_m}\right], \tag{9}$$

where N_c is the number of cells within one modulation period. The modulation wavelength has been neglected in regard to the electron mean free path. Thus, the relevant parameters to fit Eq. (9) to the experimental data are λ_m and A_n.

Setting $\lambda_m=10$, 100, 1000 Å and $A_n=10^{-3}$, 10^{-2} Å, the fit is not improved. The oscillation amplitudes are only changed if $A_n=10^{-1}$ Å. But it is unrealistic to choose such a large A_n value. So, we conclude that an ionic sinusoidal modulation cannot by itself account for both the Debye-Waller factor maximum and the amplitude misfit.

Thus, we have to introduce an electronic contribution. This can be done in Eq. (4) either with the electron mean free path or within the backscattering amplitude factor f_0.

An increase of the electron mean free path should affect all the atomic contributions. But, this is incompatible with the observation that there is no change of the Sr- and Ti-ion contributions.

One could think about a distortion of oxygen orbitals toward titanium, an effect which is known in ferroelectric perovskites (hybridization between orbitals Ti $3d$ and O $2p$),[16] creating an increase of the backscattering amplitude factor. However, there is actually no reason why this orbital hybridization has to be extremum at a temperature close to 30 K.

So, we conclude that the observed anomalies of the oscillation amplitudes cannot be explained by a small change in Eq. (4) based on a quasiharmonic approximation. Moreover, our observations must be connected with the other anomalies recently observed in the TA-phonon branches,[17] in internal friction, and in elastic compliance[18] in this temperature range.

Another unresolved point is the origin of the maximum disordered state in this temperature range (Fig. 4). If this disorder arises only from ionic motions within the tetragonal $SrTiO_3$ lattice, one has to go beyond a quasiharmonic model. This can be achieved using an order-disorder picture for the linear displacements of titanium versus its oxygen cage. In such a case, there are several equilibrium positions for the Ti ions and thus several Ti-O distances. This would increase the Debye-Waller factor at the temperature where the disorder is maximum.

However, we cannot exclude an extrinsic effect due to unwanted impurities. An extrinsic disorder, often observed in perovskites, may arise from randomly distributed centers such as oxygen vacancies[19] or Ti^{3+}. In potassium tantalate ($KTaO_3$) a dielectric loss anomaly was reduced in a fully oxidized sample.[20] We also note that an anomalous maximum of the oxygen Debye-Waller factor has been evidenced in other nonstoichiometric compounds such as $YBa_2Cu_3O_{7-\delta}$.[21]

IV. CONCLUSION

We have measured EXAFS spectra of $SrTiO_3$ at the titanium K edge. The antiferrodistortive transition at 105 K is clearly seen.

The most salient feature is a strong maximum of the oxygen Debye-Waller factor at about 31 K. This maximum has been evidenced during two separate runs, and no such effect was found in TiO_2 powders. An anomalous variation of the amplitude of the EXAFS oscillations is also found in the same temperature range. A quasiharmonic model with a sinusoidal modulation of the Ti-O distances cannot by itself fit the EXAFS data. It is necessary to introduce electronic contributions. These could arise either from unwanted impurities or from oxygen electronic-shell motion. In this respect, *ab initio* calculations would help understand the possible oxygen-orbital distortions. To settle the impurity contribution, further EXAFS experiments are planned, on compounds containing several heterovalent impurities.

[1]Y. Yacoby, J. Mustre-Deleon, E. A. Stern, J. J. Rehr, and B. Rachav, Phys. Rev. B **42**, 10 843 (1990).

[2]V. D. Klink, J. J. Rods, and S. Châtelain, Phys. Rev. B **33**, 2084 (1986).

[3]H. Uwe, K. B. Lyons, H. L. Carter, and P. A. Fleury, Phys. Rev. B **33**, 6436 (1986).

[4]Y. Yacoby and E. A. Stern, Ferroelectrics **125**, 263 (1992).

[5]Minsoo Joo, A. Edwards, Q. Islam, and D. Sayers, in *X-ray Absorption Fine Structure,* edited by S. S. Hasnain (Ellis Horwood, Chichester, 1991), p. 420.

[6]M. Fischer, B. Bonello, J. P. Itié, A. Polian, E. Dartyge, and A. Fontaine, *L.U.R.E. Rapport d'activité 1989–1992* (Edition SDEM CE SACLAY, Orsay, 1993), Vol. 2, p. 153.

[7]M. Fischer, B. Bonello, A. Polian, and J. M. Léger, in *Perovskite,* edited by A. Navrotsky and D. J. Weidner, AGU Monograph No. 45 (American Geophysical Union, Washington, D.C., 1989), p. 125.

[8]M. Fischer, B. Bonello, J. P. Itié, A. Polian, E. Dartyge, A. Fontaine, and H. Tolentino, Phys. Rev. B **42**, 8494 (1990).

[9]A. San Miguel, Thèse de l'Université P. M. Curie, 1993.

[10]F. Lyttle, J. Appl. Phys. **35**, 2212 (1964).
[11]G. Benni and P. M. Platzman, Phys. Rev. B **14**, 1514 (1976).
[12]W. Böhmer and P. Rabe, J. Phys. C **12**, 2465 (1979).
[13]W. Rehwald, Solid State Commun. **8**, 1483 (1970).
[14]S. W. Kieffer, Rev. Geophys. Space Phys. **17**, 1 (1979).
[15]S. L. Mair, J. Phys. C **19**, 6321 (1986).
[16]R. E. Cohen and H. Krakauer, Phys. Rev. B **42**, 6418 (1990).
[17]R. Vacher, J. Pelous, B. Hennion, G. Coddens, E. Courtens, and K. A. Müller, Europhys. Lett. **17**, 45 (1992).
[18]O. M. Nes, K. A. Müller, T. Suzuki, and K. Fossheim, Europhys. Lett. **129**, 397 (1992).
[19]M. Maglione, Ferroelectrics **137**, 113 (1992).
[20]S. Jandl, P. Grenier, and L. A. Boatner, Ferroelectrics **107**, 73 (1990).
[21]H. Maruyama, T. Ishii, N. Bamba, H. Madea, A. Koizumi, Y. Yoshikawa, and H. Yamazaki, Physica C **160**, 524 (1989).